Floribunda 9 (2) 2026: 67 — 80
https://ejournal.brin.go.id/floribunda/
DOI: 10.55981/floribunda.2026.16788
P-ISSN : 0215 - 4706, E-ISSN : 2460 - 6944

Comparative Evaluation of DNA Barcodes for Taxonomic Identification of Three Indonesian *Amorphophallus* Species

Sulthan Rafi Abyan Hidayat[1], Diah Ayu NurFadilah[2] & Isna Arofatun Nikmah[1,3]

1 Department of Biology, Faculty of Military Mathematics and Natural Sciences, Indonesia Defense University, Bogor, Indonesia
2 Department of Statistics, Faculty of Science and Data Analytics, Sepuluh Nopember Institute of Technology, Surabaya, Indonesia
3 Tumbuhan Asli Nusantara Foundation, BTN Korpri Blok C1 No 96, Kawatuna, Mantikulore, Palu, Sulawesi Tengah 94233, Indonesia
Correspondence: isna.nikmah@idu.ac.id

Received 30 September 2026; revised 11 October 2026; accepted 12 October 2026; available online; October published

ABSTRACT

Sulthan Rafi Abyan Hidayat, Diah Ayu NurFadilah & Isna Arofatun Nikmah 2026. Evaluasi Perbandingan Barcode DNA untuk Identifikasi Taksonomi Tiga Spesies *Amorphophallus* Indonesia. Floribunda 9(2) 67 — 80 — *Amorphophallus* Blume ex Decne. (Araceae) merupakan tumbuhan asli Indonesia yang memiliki nilai ekologis dan ekonomis penting, sehingga metode molekuler yang andal untuk identifikasi taksonomi sangat diperlukan. Sekuens GenBank dari tiga penanda plastid (*rbcL*, *matK*, dan *trnL*) dari tiga spesies *Amorphophallus* Indonesia (*A. muelleri* Blume, *A. paeoniifolius* (Dennst.) Nicolson, dan *A. titanum* (Becc.) Becc.) dianalisis menggunakan analisis celah barcoding dan pengelompokan berbasis jarak Neighbor-Joining (NJ). Ketiga penanda menunjukkan celah barcoding positif dan mengelompokkan aksesi sespesies ke dalam kluster terpisah yang sesuai dengan masing-masing spesies. *rbcL* menunjukkan celah barcoding terbesar (0,01163), diikuti oleh *trnL* (0,00873) dan *matK* (0,00278), sedangkan dukungan bootstrap untuk kluster spesies sama tingginya pada *rbcL* dan *matK* (≥95%) dan lebih rendah pada *trnL* (62–95%). Temuan ini menunjukkan *rbcL* sebagai penanda paling informatif di antara ketiga penanda yang diuji untuk identifikasi taksonomi ketiga spesies *Amorphophallus* tersebut, dengan *matK* sebagai alternatif yang sama andalnya dan *trnL* sebagai pelengkap, serta memberikan rujukan molekuler untuk kerja taksonomi dan konservasi genus ini di Indonesia selanjutnya.

Kata kunci: *Amorphophallus, barcoding gap, DNA barcoding, Kimura 2-parameter,* Neighbor-Joining

Sulthan Rafi Abyan Hidayat, Diah Ayu NurFadilah & Isna Arofatun Nikmah 2026. Comparative Evaluation of DNA Barcodes for Taxonomic Identification of Three Indonesian *Amorphophallus* Species. Floribunda 9(2) 67 — 80 — *Amorphophallus* Blume ex Decne. (Araceae) is native to Indonesia and holds significant ecological and economic value, making a reliable molecular method for taxonomic identification essential. GenBank sequences of three plastid markers (*rbcL*, *matK*, and *trnL*) from three Indonesian *Amorphophallus* species (*A. muelleri* Blume, *A. paeoniifolius* (Dennst.) Nicolson, and *A. titanum* (Becc.) Becc.) were analysed using barcoding gap analysis and Neighbor-Joining (NJ) distance-based clustering. All three markers showed a positive barcoding gap and

ISSN 0215-4706 (print) | e-ISSN 2460-6944 (online) |© 2026 The Author(s). Published by BRIN Publishing
This work is licensed under a Creative Commons Attribution-NonCommercial-ShareAlike 4.0 International License. (https://creativecommons.org/licenses/by-nc-sa/4.0)

grouped conspecific accessions into distinct clusters corresponding to each species. *rbcL* showed the largest barcoding gap (0.01163), followed by *trnL* (0.00873) and *matK* (0.00278), while bootstrap support for the species clusters was comparably high for *rbcL* and *matK* (≥95%) and lower for *trnL* (62–95%). These findings identify *rbcL* as the most informative marker among the three tested for the taxonomic identification of these three *Amorphophallus* species, with *matK* as a comparably reliable alternative and *trnL* as a complement, and provide a molecular reference for future taxonomic and conservation work on this genus in Indonesia.

Keywords: *Amorphophallus*, barcoding gap, DNA barcoding, Kimura 2-parameter, Neighbor-Joining

INTRODUCTION

Amorphophallus Blume ex Decne. (Araceae) is native to Indonesia and holds substantial ecological and economic importance: *Amorphophallus titanum* (Becc.) Becc., the titan arum, is classified as Endangered on the IUCN Red List, while *Amorphophallus muelleri* Blume and *Amorphophallus paeoniifolius* (Dennst.) Nicolson are widely cultivated for their gluco-mannan-rich corms (Mutaqin et al., 2021; Nurhidayati et al., 2024). However, morphology-based taxonomic identification within the genus is often unreliable when only seedlings, dormant corms, or processed corm material are available, because the diagnostic floral characters are ephemeral and leaves are absent for part of the growth cycle. A reliable molecular method for taxonomic identification is therefore essential to support conservation efforts.

Amorphophallus belongs to the family Araceae, subfamily Aroideae, and the monotypic tribe Thomsonieae. The genus has accumulated a complex synonymy reflecting a long and unsettled taxonomic history; several segregate genera erected by earlier authors are now treated as synonyms, and at the species level *A. paeoniifolius* alone carries more than 30 heterotypic and homotypic synonyms. Early infrageneric classification based on leaflet and inflorescence morphology was later shown to be largely artificial once molecular data became available. Combined molecular phylogenetic analyses using plastid (*trnL*, *rbcL*) and nuclear (*LEAFY* second intron) markers have demonstrated that several morphology-based infrageneric groups within *Amorphophallus* are not monophyletic (Sedayu et al. 2010; Nikmah et al. 2016). Claudel et al. (2017) subsequently proposed a revised infrageneric classification of four subgenera using *rbcL*, *matK*, and nuclear *ITS1* data, under which *A. titanum* is placed among giant-inflorescence species allied with *A. gigas* and *A. hewittii*, while *A. muelleri* and *A. paeoniifolius* belong to separate, more distantly related lineages despite their superficial similarity as cultivated, glucomannan-producing crops. This history of extensive synonymy underscores why molecular data are increasingly considered necessary to support morphology-based taxonomy in this genus (Li et al., 2024).

DNA barcoding using short, standardized plastid regions such as *rbcL*, *matK*, and *trnL* has been widely applied for plant taxonomic identification (Hebert et al., 2003; CBOL Plant Working Group, 2009; Taberlet et al., 2007; Nair et al., 2024), with alternative marker combinations such as *rbcL* plus the non-coding *trnH-psbA* spacer also proposed for broader taxonomic applicability (Kress & Erickson, 2007). However, marker effectiveness varies considerably across plant lineages and must be evaluated within each target taxonomic group rather than assumed from unrelated studies (Elansary et al., 2017; Braukmann et al., 2017; Wei et al., 2024). Marker performance is commonly assessed via the barcoding gap, the difference between the minimum interspecific and maximum intraspecific genetic distance under the Kimura 2-parameter (K2P) model (Meyer & Paulay, 2005; Kimura, 1980), with a positive gap indicating reliable species-level discrimination. To date, no study has evaluated the comparative performance of *rbcL*, *matK*, and *trnL* specifically for Indonesian *Amorphophallus*.

This study therefore evaluates the effectiveness of *rbcL*, *matK*, and *trnL* for the taxonomic identification of three Indonesian *Amorphophallus* species, *A. muelleri*, *A. paeoniifolius*, and *A. titanum*, using publicly available

GenBank sequences. Specifically, it aims to: (1) assess the barcoding gap of each marker, (2) evaluate the clustering of conspecific accessions and its bootstrap support in Neighbor-Joining trees for each marker, and (3) identify which of the three markers is most suitable for supporting morphology-based taxonomy of this genus with molecular evidence. These three species were selected because multiple GenBank accessions of all three markers are available for each of them, allowing marker performance to be compared on the same species set, and because together they represent the principal economic and conservation interests in the genus in Indonesia: *A. muelleri* and *A. paeoniifolius* as cultivated corm crops and *A. titanum* as an Endangered species. Although mature plants of the three species can be distinguished morphologically, a validated molecular reference for this species set is of practical value where diagnostic organs are absent, such as for seedlings, dormant corms, processed corm products, and herbarium vouchers lacking leaves or floral organs.

MATERIALS AND METHODS

Sequence Acquisition

Nucleotide sequences for three plastid markers, *rbcL*, *matK*, and *trnL*, were retrieved from the National Center for Biotechnology Information (NCBI) GenBank database (NCBI GenBank) for three *Amorphophallus* species: *A. muelleri*, *A. paeoniifolius*, and *A. titanum*. A total of 13 *matK* sequences, 11 *rbcL* sequences, and 12 *trnL* sequences were compiled across the three species (Table 1). Sequences originated from heterogeneous submission types, including partial coding sequence (CDS) entries and longer fragments spanning the *trnK* intron plus *matK* complete CDS, or the complete *rbcL* gene, reflecting the variation typical of publicly deposited GenBank records for non-model taxa. Species identity for each accession was verified against the taxonomic name, submitting institution, and, where available, the voucher specimen cited in the GenBank record; several accessions cite herbarium voucher specimens (for example, K for the Royal Botanic Gardens, Kew, and NMNH for the Smithsonian National Museum of Natural History), providing an independent basis for confirming correct species identity beyond the submitter's original label. Accessions were additionally screened for the presence of non-standard IUPAC ambiguity codes prior to alignment.

Sequence Alignment and Trimming

Multiple sequence alignment was performed independently for each marker using ClustalW v2.1 (Larkin et al. 2007) with default parameters (gap opening penalty = 10, gap extension penalty = 0.2, DNA weight matrix = IUB). Because sequences within each marker set differed substantially in length and genomic span, raw alignments retained large terminal gap regions corresponding to sequence segments not shared across all accessions. To ensure that genetic distance comparisons were not biased by missing data at alignment termini, each alignment was trimmed to the region of full mutual overlap, defined as the contiguous block of alignment columns in which every accession contributed an unambiguous nucleotide call. For *matK* and *rbcL*, this overlap region was free of internal indels, yielding gapless trimmed alignments of 729 bp (*matK*, n = 13) and 522 bp (*rbcL*, n = 11), respectively. For *trnL*, the overlap region contained genuine internal indels attributable to length polymorphism within the intron, consistent with previously documented indel-rich behaviour of this locus (Taberlet et al. 2007); the largest indel-free contiguous block within this overlap (231 bp, n = 12) was used as the primary trimmed alignment to maintain methodological consistency with *matK* and *rbcL*. As a sensitivity check, a second *trnL* alignment retaining the full overlap region including indels (385 bp) was also analysed using pairwise deletion of gap positions; both approaches yielded a positive barcoding gap, and results from the primary gapless alignment are reported unless otherwise noted.

Genetic Distance and Barcoding Gap Analysis

Pairwise genetic distances were calculated for each trimmed alignment using the Kimura 2-parameter (K2P) substitution model (Kimura 1980) in MEGA12 (Kumar et al. 2024). K2P was chosen because it is the distance model conventionally used in DNA barcoding studies

ISSN 0215-4706 (print) | e-ISSN 2460-6944 (online) |© 2026 The Author(s). Published by BRIN Publishing
This work is licensed under a Creative Commons Attribution-NonCommercial-ShareAlike 4.0 International License.
(https://creativecommons.org/licenses/by-nc-sa/4.0)

(Hebert et al. 2003), which allows the barcoding gap values reported here to be compared directly with published barcoding studies, and because it corrects for the higher rate of transitions relative to transversions while remaining adequate at the low levels of divergence observed here (≤2.4%), at which more parameter-rich substitution models yield nearly identical distance estimates. For each marker, intraspecific distances (pairwise comparisons within the same species) and interspecific distances (pairwise comparisons between different species) were extracted from the full pairwise distance matrix. The barcoding gap was calculated following Meyer and Paulay (2005) as:

Barcoding gap = minimum interspecific distance − maximum intraspecific distance

A positive barcoding gap value indicates the absence of overlap between intraspecific and interspecific variation, supporting reliable species discrimination for that marker.

Genetic Distance-Based Clustering

Neighbor-Joining (NJ) trees (Saitou & Nei 1987) were constructed independently for each trimmed marker alignment based on K2P genetic distances. Clade support was assessed using 1,000 bootstrap replicates following the resampling procedure of Felsenstein (1985), generated by resampling alignment columns with replacement and recalculating the NJ topology for each pseudoreplicate; bootstrap support values were then mapped onto the corresponding nodes of the best NJ tree (Felsenstein 1985). Trees were rooted at the midpoint for display. Bootstrap support is reported for the bipartition defining each species cluster, calculated as the proportion of bootstrap trees in which the accessions of that species formed a separate cluster. NJ was used rather than maximum likelihood (ML) because the purpose of this analysis was not to infer evolutionary relationships among the species but to test whether conspecific accessions cluster together on the basis of the same K2P distances used for the barcoding gap, which is the conventional tree-based criterion in DNA barcoding (Hebert et al. 2003; Trujillo-Argueta et al. 2022). Because only three species were sampled and no outgroup was included, the trees are interpreted as distance-based clustering diagrams rather than as phylogenetic hypotheses.

Software and Reproducibility

Sequence alignment was performed in ClustalW v2.1 (Larkin et al. 2007). Genetic distances and barcoding gaps were computed independently in MEGA12 (Kumar et al. 2024) and in a custom Python 3 pipeline built on Biopython (Cock et al. 2009) implementing the K2P model, and the results were cross-validated between the two platforms to confirm numerical consistency prior to interpretation. Neighbor-Joining trees, bootstrap resampling (1,000 replicates, random seed 2026), and species-cluster support were computed in R 4.3.3 (R Core Team 2024) using the package ape (Paradis & Schliep 2019); trees were midpoint-rooted with phangorn (Schliep 2011) and drawn with ggtree (Yu et al. 2017).

Table 1. GenBank accessions used for *matK*, *rbcL*, and *trnL* sequence analysis in three *Amorphophallus* species.

Marker	Species	Accession No.	Raw Length (bp)	Description
matK	*A. muelleri*	MT850200.1	834	Partial CDS, clone 2
matK	*A. muelleri*	MT850201.1	834	Partial CDS, clone 3
matK	*A. muelleri*	MT850202.1	834	Partial CDS, clone 4
matK	*A. muelleri*	MT850203.1	834	Partial CDS, clone 5
matK	*A. muelleri*	MT850204.1	834	Partial CDS, clone 6

Table 1. GenBank accessions used for *matK*, *rbcL*, and *trnL* sequence analysis in three *Amorphophallus* species. (*continue*)

Marker	Species	Accession No.	Raw Length (bp)	Description
matK	*A. muelleri*	AF387406.1	1802	*trnK* intron + *matK* complete CDS
matK	*A. paeoniifolius*	AF387410.1	1795	*trnK* intron + *matK* complete CDS
matK	*A. paeoniifolius*	PP921943.1	864	Partial CDS, voucher KM 0105/24
matK	*A. paeoniifolius*	MW035333.1	738	Partial CDS, var. *paeoniifolius*
matK	*A. titanum*	KY490466.1	1787	Complete CDS, isolate AM27
matK	*A. titanum*	KY490479.1	1781	Complete CDS, isolate AM116
matK	*A. titanum*	AF387421.1	1785	*trnK* intron + *matK* complete CDS
matK	*A. titanum*	AJ581391.1	808	Partial CDS, voucher Chase 2968
rbcL	*A. muelleri*	MT850225.1	683	Partial CDS, clone 2
rbcL	*A. muelleri*	MT850226.1	683	Partial CDS, clone 3
rbcL	*A. muelleri*	MT850227.1	683	Partial CDS, clone 4
rbcL	*A. muelleri*	MT850228.1	683	Partial CDS, clone 5
rbcL	*A. muelleri*	MT850229.1	683	Partial CDS, clone 6
rbcL	*A. muelleri*	EF590499.1	543	Partial CDS, voucher NMNH 96-216
rbcL	*A. paeoniifolius*	PX853368.1	578	Partial CDS, isolate NFB033
rbcL	*A. paeoniifolius*	PX853369.1	577	Partial CDS, isolate NFB035
rbcL	*A. paeoniifolius*	PP921944.1	678	Partial CDS, voucher KM 0105/24
rbcL	*A. titanum*	AF497102.1	1466	Complete/long CDS
rbcL	*A. titanum*	EF590500.1	544	Partial CDS, voucher NMNH 03-142
trnL	*A. muelleri*	KR534378.1	962	Partial sequence, isolate MU-TK02
trnL	*A. muelleri*	KR534379.1	930	Partial sequence, isolate MU-TK01
trnL	*A. muelleri*	KR534380.1	835	Partial sequence, isolate MU-ME01
trnL	*A. muelleri*	KR534381.1	978	Partial sequence, isolate MU-ME02
trnL	*A. muelleri*	KR534382.1	961	Partial sequence, isolate MU-KC01
trnL	*A. muelleri*	KR534383.1	980	Partial sequence, isolate MU-KC02
trnL	*A. paeoniifolius*	AF387464.1	563	Partial sequence
trnL	*A. paeoniifolius*	MN844024.1	401	Intron
trnL	*A. paeoniifolius*	KY887282.1	371	Intron, isolate MXXZ_14
trnL	*A. paeoniifolius*	KY887283.1	371	Intron, isolate MXXZ_11
trnL	*A. titanum*	AF387474.1	583	Partial sequence
trnL	*A. titanum*	AY555180.1	962	Partial sequence, voucher Barabe & Archambault 199

ISSN 0215-4706 (print) | e-ISSN 2460-6944 (online) |© 2026 The Author(s). Published by BRIN Publishing
This work is licensed under a Creative Commons Attribution-NonCommercial-ShareAlike 4.0 International License.
(https://creativecommons.org/licenses/by-nc-sa/4.0)

Table 2. Summary of raw and trimmed alignment lengths for each marker.

Marker	n	Raw Alignment Length (bp)	Trimmed Length (bp)	Internal Indels in Trimmed Region
matK	13	1,820	729	None (gapless block)
rbcL	11	1,471	522	None (gapless block)
trnL	12	1,030	231	None (gapless block; largest indel-free segment of a 385 bp overlap region)

RESULTS AND DISCUSSION

Sequence Alignment and Trimming

ClustalW alignment of the 13 *matK*, 11 *rbcL*, and 12 *trnL* sequences produced raw alignments of 1,820 bp, 1,471 bp, and 1,030 bp, respectively, reflecting the heterogeneous length and genomic span of the source GenBank records (partial coding sequences ranging from 371–864 bp alongside longer *trnK*-intron-inclusive or complete-gene records of up to 1,802 bp). Trimming each alignment to the region of full mutual overlap yielded a 729 bp gapless block for *matK* (n = 13), a 522 bp gapless block for *rbcL* (n = 11), and a 231 bp gapless block for *trnL* (n = 12). For *matK* and *rbcL*, the full-overlap region contained no internal indels, indicating that all length variation among accessions originated from differences in sequencing/submission span rather than genuine insertion–deletion events. For *trnL*, the full-overlap region (385 bp) contained 59 alignment columns with internal gaps, consistent with the known length polymorphism of the *trnL* intron; the largest indel-free segment within this region (231 bp) was retained as the primary trimmed alignment, while the full 385 bp overlap (analysed with pairwise deletion of gaps) was retained as a sensitivity comparison (Table 2).

Genetic Distance and Barcoding Gap

Pairwise K2P genetic distances were computed for each trimmed alignment (Table 3, Table 4). All three markers exhibited a positive barcoding gap, indicating the theoretical capacity of each locus to discriminate the three *Amorphophallus* species without overlap between intraspecific and interspecific variation.

For *matK*, intraspecific distances ranged from 0.00000 (identical sequences within *A. muelleri* and within *A. titanum*) to a maximum of 0.00828, the latter driven by minor sequence divergence among *A. paeoniifolius* accessions (specifically MW035333.1 relative to AF387410.1 and PP921943.1). The minimum interspecific distance was 0.01106, observed between *A. paeoniifolius* and *A. titanum*, yielding a barcoding gap of 0.00278.

For *rbcL*, all accessions within each species were genetically identical across the 522 bp trimmed region (intraspecific distance = 0.00000 for all three species). The minimum interspecific distance was 0.01163, also between *A. paeoniifolius* and *A. titanum*, yielding a barcoding gap of 0.01163, the largest among the three markers evaluated.

For *trnL*, intraspecific distances were likewise 0.00000 across all three species in the 231 bp gapless alignment. The minimum interspecific distance was 0.00873, observed between *A. muelleri* and *A. titanum*, yielding a barcoding gap of 0.00873. When the sensitivity analysis retaining *trnL* indels (385 bp, pairwise deletion) was considered instead, the barcoding gap increased to 0.01516, indicating that indel information contributes additional discriminatory signal beyond nucleotide substitutions alone; this pattern is consistent with the intron origin of *trnL*, where insertion–deletion events accumulate alongside point substitutions.

Ranked by barcoding gap magnitude, the three markers performed as follows: *rbcL* (0.01163) > *trnL* (0.00873) > *matK* (0.00278) (Table 3). Across all markers, the species pair

consistently associated with the smallest interspecific distance was *A. paeoniifolius* and *A. titanum* (*matK* and *rbcL*) or *A. muelleri* and *A. titanum* (*trnL*), suggesting these species pairs represent the most challenging discrimination task for single-locus barcoding among the three species studied.

Table 3. Summary of Kimura 2-parameter (K2P) genetic distances and barcoding gap for each marker.

Marker	Max. Intraspecific Distance	Min. Interspecific Distance	Barcoding Gap	Species Pair at Min. Interspecific Distance
matK	0.00828	0.01106	0.00278	*A. paeoniifolius* vs *A. titanum*
rbcL	0.00000	0.01163	0.01163	*A. paeoniifolius* vs *A. titanum*
trnL	0.00000	0.00873	0.00873	*A. muelleri* vs *A. titanum*

Table 4. Pairwise interspecific K2P genetic distances (range or single value) by species pair and marker.

Marker	***A. muelleri* vs *A. paeoniifolius***	***A. muelleri* vs *A. titanum***	***A. paeoniifolius* vs *A. titanum***
matK	0.01526 – 0.02373	0.01246	0.01106 – 0.01948
rbcL	0.01552	0.01749	0.01163
trnL	0.01762	0.00873	0.01762

Genetic Distance-Based Clustering

Neighbor-Joining trees constructed from K2P distances for all three markers grouped the accessions into three clusters corresponding to *A. muelleri*, *A. paeoniifolius*, and *A. titanum*, with no intermixing of accessions across species boundaries (Figures 1–3). Because the aim of this analysis is species discrimination, bootstrap support is reported for the bipartition defining each species cluster, that is, for interspecific rather than intraspecific relationships (Table 5). For *matK*, support for the *A. muelleri*, *A. paeoniifolius*, and *A. titanum* clusters was 100%, 100%, and 95%, respectively; for *rbcL* it was 99%, 95%, and 99%; and for *trnL* it was 65%, 95%, and 62%. *matK* and *rbcL* therefore provided comparably strong support (≥95%) for all three species clusters, whereas *trnL* strongly supported only the *A. paeoniifolius* cluster and gave weak support to the separation of *A. muelleri* from *A. titanum*. This lower support reflects the small number of variable sites in the 231 bp *trnL* alignment (five, compared with 20 in *matK* and 11 in *rbcL*; Table 5), of which only two distinguish *A. muelleri* from *A. titanum*; with so little information, a substantial proportion of bootstrap pseudoreplicates no longer separate these two species. Nodes within each species cluster reflect branching order among identical or near-identical sequences and are not interpreted further.

ISSN 0215-4706 (print) | e-ISSN 2460-6944 (online) |© 2026 The Author(s). Published by BRIN Publishing
This work is licensed under a Creative Commons Attribution-NonCommercial-ShareAlike 4.0 International License.
(https://creativecommons.org/licenses/by-nc-sa/4.0)

Table 5. Number of variable and parsimony-informative sites in each trimmed alignment and bootstrap support (%, 1,000 replicates) for the cluster formed by each species in the Neighbor-Joining trees.

Marker	Trimmed Length (bp)	Variable Sites	Parsimony-informative Sites	Bootstrap Support: *A. muelleri* / *A. paeoniifolius* / *A. titanum*
matK	729	20	14	100 / 100 / 95
rbcL	522	11	11	99 / 95 / 99
trnL	231	5	5	65 / 95 / 62

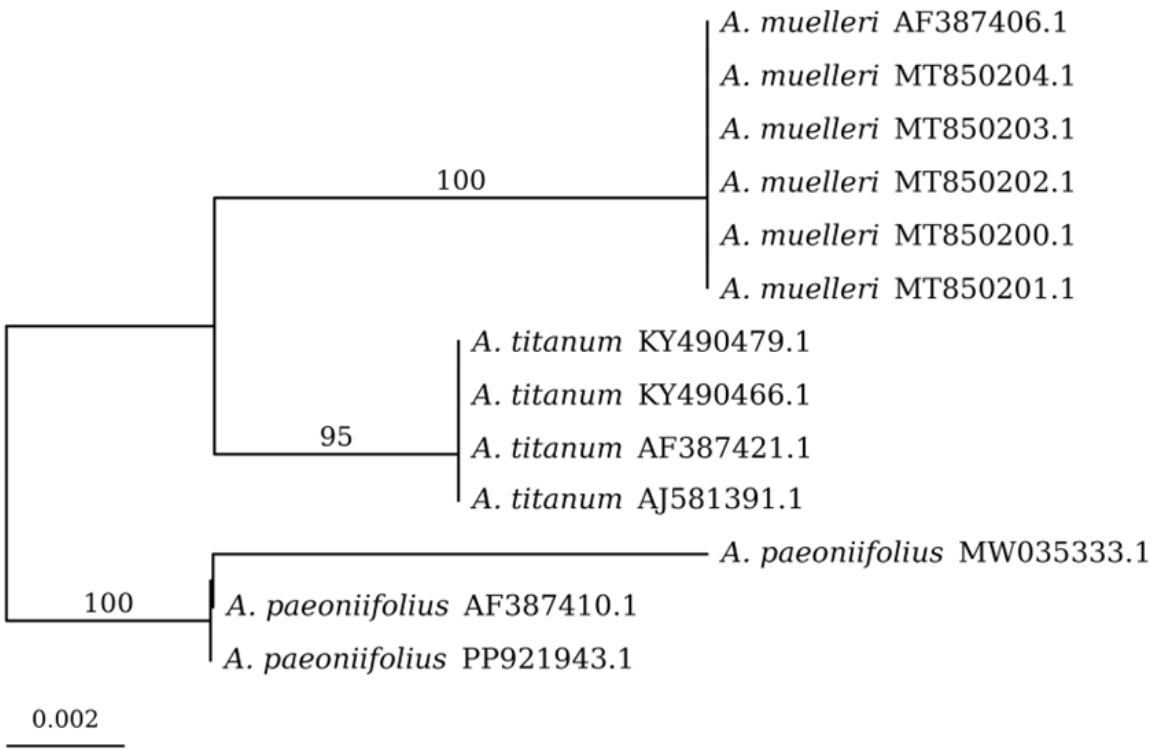


Figure 1. Neighbor-Joining tree of *Amorphophallus* based on *matK* (729 bp, K2P distance, 1,000 bootstrap replicates), midpoint-rooted and drawn with ggtree (Yu et al. 2017). Values on branches indicate bootstrap support (%) for each species cluster. Tip labels are italicized to denote binomial species names.

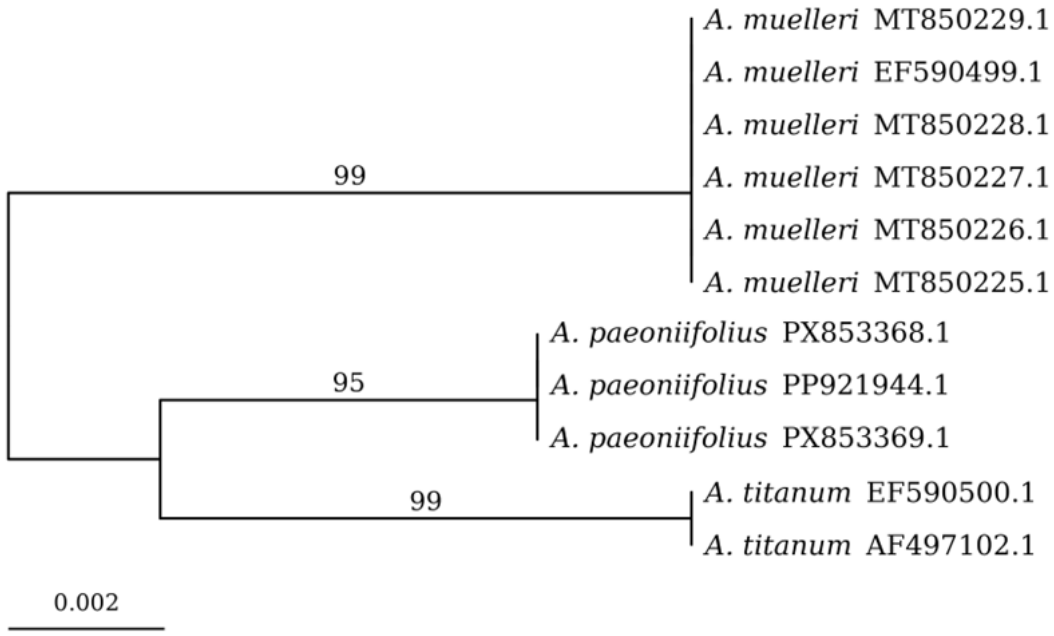


Figure 2. Neighbor-Joining tree of *Amorphophallus* based on *rbcL* (522 bp, K2P distance, 1,000 bootstrap replicates), midpoint-rooted and drawn with ggtree (Yu et al. 2017). Values on branches indicate bootstrap support (%) for each species cluster.

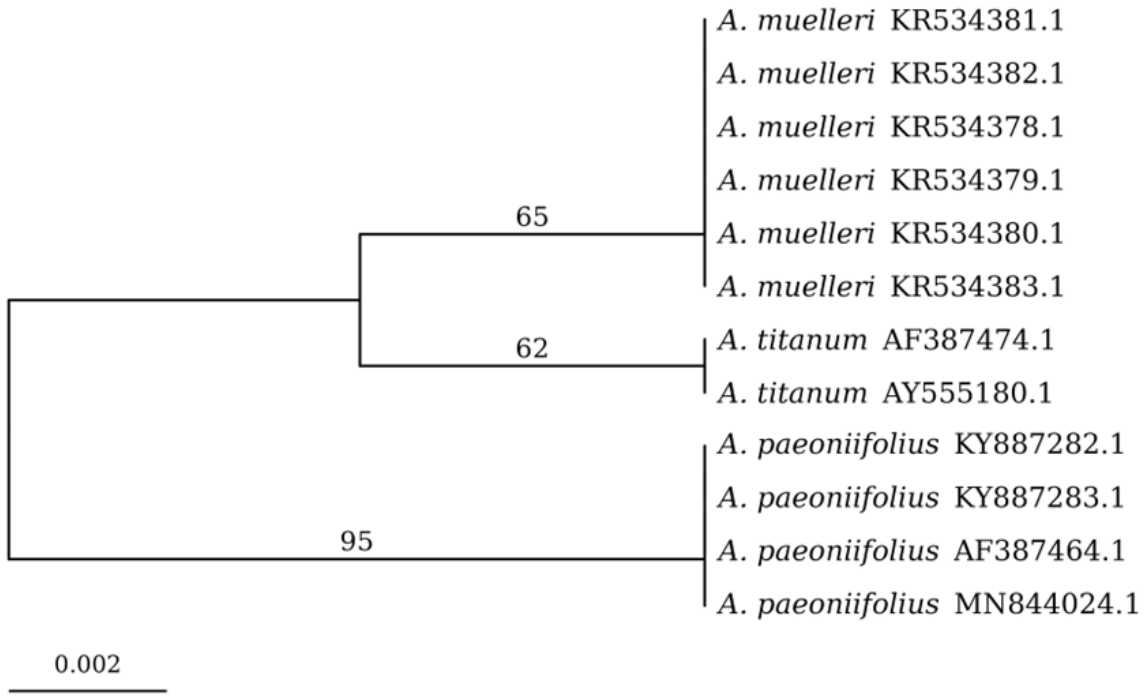


Figure 3. Neighbor-Joining tree of *Amorphophallus* based on *trnL* (231 bp gapless region, K2P distance, 1,000 bootstrap replicates), midpoint-rooted and drawn with ggtree (Yu et al. 2017). Values on branches indicate bootstrap support (%) for each species cluster.

ISSN 0215-4706 (print) | e-ISSN 2460-6944 (online) |© 2026 The Author(s). Published by BRIN Publishing
This work is licensed under a Creative Commons Attribution-NonCommercial-ShareAlike 4.0 International License.
(https://creativecommons.org/licenses/by-nc-sa/4.0)

This study demonstrates that all three plastid markers evaluated, *rbcL*, *matK*, and *trnL*, are capable of discriminating *A. muelleri*, *A. paeoniifolius*, and *A. titanum*, as evidenced by a positive barcoding gap and the clustering of conspecific accessions in Neighbor-Joining trees for every marker tested. This finding is consistent with previous DNA barcoding studies in other plant genera and taxonomic groups, which similarly report that no single locus is universally optimal, but that the core CBOL markers (*rbcL*, *matK*) combined with supplementary loci (such as *trnL*) generally provide adequate species-level resolution when sampling is sufficient (Elansary et al. 2017; Braukmann et al. 2017). This pattern of marker-dependent, family- or genus-specific performance has been repeatedly documented across unrelated plant lineages, from Cactaceae (Wei et al. 2024) to Neotropical cloud-forest floras (Trujillo-Argueta et al. 2022), reinforcing the view that barcoding marker selection should generally be validated empirically for each target group rather than assumed from prior studies on unrelated taxa.

Among the three markers, *rbcL* was the most informative for discriminating the three species studied, combining the largest barcoding gap (0.01163) with strong bootstrap support (≥95%) for all three species clusters. This result reflects the complete absence of intraspecific variation among all sampled *rbcL* accessions alongside comparatively high interspecific divergence, and is consistent with *rbcL*'s established reliability as a core barcode across many plant groups. In practice, because a DNA barcode does not depend on the presence of reproductive organs, *rbcL* could support the identification of these three species when such organs, the traditional basis for *Amorphophallus* identification, are unavailable, such as for juvenile plants, processed corm material, or herbarium specimens collected outside the brief flowering period; this application, however, remains to be tested directly with field-collected material.

matK, in contrast, showed the narrowest barcoding gap (0.00278), although its bootstrap support for the three species clusters was comparable to that of *rbcL* (Table 5). The narrow gap is driven entirely by a single *A. paeoniifolius* accession, MW035333.1, cited in GenBank as *A. paeoniifolius* var. *paeoniifolius*. Inspection of the multiple sequence alignment showed that this accession contains no indels relative to the other two *A. paeoniifolius* accessions (AF387410.1 and PP921943.1) but differs from both at six nucleotide positions, all of which are unique to MW035333.1 among the 13 *matK* sequences. All six substitutions are changes to cytosine, and five of them lie at the extreme ends of the trimmed region (positions 10, 21, 34, 35, and 726 of 729 bp): four within the first 35 bases and one within the last 13 bases of the submitted MW035333.1 sequence. Because the terminal regions of Sanger reads typically have the lowest base-calling quality, at least part of this divergence may reflect sequencing error rather than genuine intraspecific variation; true variation or a labelling inconsistency cannot, however, be excluded without access to the original chromatograms and voucher specimen. When MW035333.1 was excluded, the maximum intraspecific distance for *matK* fell to zero and the barcoding gap increased to 0.01106, comparable to that of *rbcL*. The *matK* barcoding gap reported here should therefore be regarded as a conservative estimate, and this accession is flagged for verification in future sampling of *A. paeoniifolius*.

trnL showed an intermediate barcoding gap (0.00873) but the lowest bootstrap support for species clusters (62–95%) among the three markers, reflecting its small number of variable sites (Table 5), making it the least reliable of the three for standalone taxonomic identification in this genus, though still useful as a complementary marker. This is broadly consistent with an earlier *trnL*-based assessment of *A. muelleri* population structure in East Java (Rosidiani et al. 2013), which likewise found *trnL* informative but not decisively resolving at finer taxonomic scales.

Limited intraspecific sampling, particularly for *A. titanum* (n = 2 for *rbcL* and *trnL*) and *A. paeoniifolius* (n = 3–4 across markers), represents the principal limitation of this study, echoing a broader concern raised in the DNA barcoding literature that typical per-species sample sizes

of five or fewer individuals are often insufficient to fully characterize intraspecific haplotype diversity (Phillips et al. 2019). Because barcoding gap estimates are sensitive to the range of intraspecific variation captured, the zero intraspecific distances reported here for several species–marker combinations may reflect insufficient sampling rather than genuinely absent intraspecific polymorphism. Future work incorporating population-level sampling across the geographic range of each species, particularly for *A. titanum* given its conservation status and the documented decline of its wild population (Yudaputra et al. 2022), would provide a more robust test of barcoding gap stability; comparable population-genomic approaches applied to other range-restricted *Amorphophallus* species, such as *A. albus* in China, have similarly revealed that adequate population-level sampling is essential for characterizing genetic structure in narrowly distributed taxa (Tang et al. 2020). Additionally, because the three markers differ in the number and identity of accessions available in GenBank (a practical constraint typical of non-model, conservation-priority taxa), direct comparison of absolute barcoding gap magnitudes across markers should be interpreted as indicative rather than definitive.

Because the three markers were analysed separately, the present data do not test the performance of a concatenated multi-locus barcode. Nevertheless, the complementary strengths observed here, namely the wide barcoding gap of *rbcL*, the strong cluster support and larger existing reference database of *matK*, and the additional signal carried by *trnL* indel variation, suggest that using more than one of these markers for identity verification would reduce the risk that the limitations of a single marker (whether low intrinsic variability, small reference sample size, or alignment-trimming decisions) compromise identification in applied conservation or trade-verification contexts. Formal evaluation of a combined barcode, building on the *rbcL* + *matK* core barcode recommended for land plants by the CBOL Plant Working Group (2009), remains a task for future work with larger sampling.

Taxonomic Implications

The consistent clustering of conspecific accessions and the positive barcoding gap recovered for *A. muelleri*, *A. paeoniifolius*, and *A. titanum* across all three markers are consistent with the current recognition of these taxa as distinct species. This observation should, however, be interpreted within the limits of the present dataset: only three species and a small number of accessions per species were examined, no outgroup was included, and the analysis was designed to evaluate marker discrimination rather than to test species boundaries. The results therefore do not constitute an independent test of taxonomic status, which in this genus would require broader taxon sampling given its long and complex nomenclatural history; *A. paeoniifolius* alone carries more than 30 heterotypic and homotypic synonyms. Likewise, whether infraspecific taxa, such as the varieties recognised within *A. paeoniifolius*, are genetically distinct would require dedicated sampling across the range of the species.

These findings are also compatible with the infrageneric framework proposed by Claudel et al. (2017), who used *rbcL* and *matK* together with nuclear *ITS1* data to reconstruct genus-wide relationships in a 157-species phylogeny and to delimit four *Amorphophallus* subgenera, under which *A. muelleri* and *A. paeoniifolius* belong to separate lineages. In line with this, *A. muelleri* and *A. paeoniifolius*, despite their overlapping vernacular use as cultivated glucomannan-yielding "porang"-type crops, were not the most similar species pair for any of the three markers evaluated (Table 4), indicating that agronomic or vernacular groupings should not be assumed to reflect relatedness in this genus. Relationships among the three species themselves, however, cannot be inferred from the present distance-based clustering, which included only three species and no outgroup.

From a practical taxonomic standpoint, the marker-specific barcoding gaps, numbers of variable sites (Table 5), and species-level clustering demonstrated here support the potential use of *rbcL* and *matK*, supplemented

ISSN 0215-4706 (print) | e-ISSN 2460-6944 (online) |© 2026 The Author(s). Published by BRIN Publishing
This work is licensed under a Creative Commons Attribution-NonCommercial-ShareAlike 4.0 International License.
(https://creativecommons.org/licenses/by-nc-sa/4.0)

by *trnL*, as a working molecular toolkit for routine identity verification of these three species in contexts where morphological diagnosis is impractical, such as verifying the species identity of processed corm material entering the glucomannan trade, screening seedlings or juvenile plants in nursery and reintroduction programmes, or authenticating herbarium and living collection vouchers where flowering material is unavailable. Because *Amorphophallus* taxonomy has historically relied heavily on inflorescence characters that are only present for a few days during the plant's multi-year growth cycle, a molecular reference dataset of the kind assembled here, once validated with field-collected material, could provide an identification resource that does not depend on the life stage of the plant.

CONCLUSION

This study compared *rbcL*, *matK*, and *trnL* for the taxonomic identification of three Indonesian *Amorphophallus* species. All three markers showed a positive barcoding gap and grouped conspecific accessions into distinct species clusters, consistent with the current recognition of these three species. *rbcL* showed the largest barcoding gap (0.01163), followed by *trnL* (0.00873) and *matK* (0.00278); *rbcL* and *matK* provided comparably strong bootstrap support for all species clusters (≥95%), whereas *trnL* provided weaker support (62–95%). *rbcL* is therefore the most informative of the three markers for discriminating these three species, with *matK* as a comparably reliable alternative whose narrow barcoding gap is attributable to a single divergent accession. Because the markers were analysed separately and intraspecific sampling was limited, the performance of a combined multi-locus barcode and the applicability of these results to other *Amorphophallus* species remain to be tested. These findings provide a molecular reference for future taxonomic and conservation work on *Amorphophallus* in Indonesia.

REFERENCES

Braukmann TWA, Kuzmina ML, Sills J, Zakharov EV & Hebert PDN 2017. Testing the efficacy of DNA barcodes for identifying the vascular plants of Canada. *PLoS ONE* 12(1): e0169515.

CBOL Plant Working Group 2009. A DNA barcode for land plants. *Proceedings of the National Academy of Sciences* 106(31): 12794–12797.

Claudel C, Buerki S, Chatrou LW, Antonelli A, Alvarez N & Hetterscheid W 2017. Large-scale phylogenetic analysis of *Amorphophallus* (Araceae) derived from nuclear and plastid sequences reveals new subgeneric delineation. *Botanical Journal of the Linnean Society* 184(1): 32–45.

Cock PJA, Antao T, Chang JT, Chapman BA, Cox CJ, Dalke A, Friedberg I, Hamelryck T, Kauff F, Wilczynski B & de Hoon MJL 2009. Biopython: freely available Python tools for computational molecular biology and bioinformatics. *Bioinformatics* 25(11): 1422–1423.

Elansary HO, Ashfaq M, Ali HM & Yessoufou K 2017. The first initiative of DNA barcoding of ornamental plants from Egypt and potential applications in horticulture industry. *PLoS ONE* 12(2): e0172170.

Felsenstein J 1985. Confidence limits on phylogenies: an approach using the bootstrap. *Evolution* 39(4): 783–791.

Hebert PDN, Cywinska A, Ball SL & deWaard JR 2003. Biological identifications through DNA barcodes. *Proceedings of the Royal Society B: Biological Sciences* 270(1512): 313–321.

Kimura M 1980. A simple method for estimating evolutionary rates of base substitutions through comparative studies of nucleotide sequences. *Journal of Molecular Evolution* 16 (2): 111–120.

Kress WJ & Erickson DL 2007. A two-locus global DNA barcode for land plants: the coding *rbcL* gene complements the non-coding *trnH-psbA* spacer region. *PLoS ONE* 2(6): e508.

Kumar S, Stecher G, Suleski M, Sanderford M, Sharma S & Tamura K 2024. MEGA12: molecular evolutionary genetics analysis version 12 for adaptive and green computing. *Molecular Biology and Evolution* 41(12): msae263.

Larkin MA, Blackshields G, Brown NP, Chenna R, McGettigan PA, McWilliam H, Valentin F, Wallace IM, Wilm A, Lopez R, Thompson JD, Gibson TJ & Higgins DG 2007. Clustal W and Clustal X version 2.0. *Bioinformatics* 23(21): 2947–2948.

Li LF, Yang M, Qi Y, Gao PH, Yang SW, Zhao YT, Guo JW, Wei HY, Liu JN, Zhao JR, Huang FY & Yu L 2024. Chloroplast genome of four *Amorphophallus* species: genomic features, comparative analysis, and phylogenetic relationships among *Amorphophallus* species. *BMC Genomics* 25(1): 1122.

Meyer CP & Paulay G 2005. DNA barcoding: error rates based on comprehensive sampling. *PLOS Biology* 3(12): e422.

Mutaqin AZ, Kurniadie D, Iskandar J, Nurzaman M & Husodo T 2021. Morphological characteristics and habitat conditions of suweg (*Amorphophallus paeoniifolius*) around Mount Ciremai National Park, West Java, Indonesia. *Biodiversitas Journal of Biological Diversity* 22(5): 2591–2600.

Nair VD, Aseema P & Saini KC 2024. DNA barcoding: an effective molecular tool for species identification, molecular authentication and phylogeny studies in plant science research. *Plant Science Today* 11(4).

Nikmah IA, Azrianingsih R & Wahyudi D 2016. Genetic diversity of porang populations (*Amorphophallus muelleri* Blume) in Central Java and West Java based on *LEAFY* second intron marker. *The Journal of Tropical Life Science* 6(1): 23–27.

Nurhidayati T, Febriawan Z, Saputro TB, Arifiyanto A & Purwani KI 2024. Morpho-physiological and glucomannan biosynthesis-related gene expression of porang (*Amorphophallus muelleri* Blume) under salinity stress. *Acta Botanica Brasilica* 38: e20230222.

Paradis E & Schliep K 2019. ape 5.0: an environment for modern phylogenetics and evolutionary analyses in R. *Bioinformatics* 35 (3): 526–528.

Phillips JD, Gillis DJ & Hanner RH 2019. Incomplete estimates of genetic diversity within species: implications for DNA barcoding. *Ecology and Evolution* 9(5): 2996 –3010.

R Core Team 2024. R: a language and environment for statistical computing. R Foundation for Statistical Computing, Vienna, Austria.

Rosidiani EP, Arumingtyas EL & Azrianingsih R 2013. Analisis variasi genetik *Amorphophallus muelleri* Blume dari berbagai populasi di Jawa Timur berdasarkan sekuen intron *trnL*. *Floribunda* 4(6): 129–137.

Saitou N & Nei M 1987. The neighbor-joining method: a new method for reconstructing phylogenetic trees. *Molecular Biology and Evolution* 4(4): 406–425.

Schliep KP 2011. phangorn: phylogenetic analysis in R. *Bioinformatics* 27(4): 592–593.

Sedayu A, Eurlings MCM, Gravendeel B & Hetterscheid WLA 2010. Morphological character evolution of *Amorphophallus* (Araceae) based on a combined phylogenetic analysis of *trnL, rbcL* and *LEAFY* second intron sequences. *Botanical Studies* 51(4): 473–490.

Taberlet P, Coissac E, Pompanon F, Gielly L, Miquel C, Valentini A, Vermat T, Corthier G, Brochmann C & Willerslev E 2007. Power and limitations of the chloroplast *trnL* (UAA) intron for plant DNA barcoding. *Nucleic Acids Research* 35(3): e14.

Tang R, Liu E, Zhang Y, Schinnerl J, Sun W & Chen G 2020. Genetic diversity and population structure of *Amorphophallus albus*, a plant species with extremely small populations (PSESP) endemic to dry-hot valley of Jinsha River. *BMC Genetics* 21(1): 102.

Trujillo-Argueta S, Del Castillo RF & Velasco-Murguía A 2022. Testing the effectiveness of *rbcLa* DNA-barcoding for species discrimination in tropical montane cloud forest vascular plants (Oaxaca, Mexico) using BLAST, genetic distance, and tree-based methods. *PeerJ* 10: e13771.

Wei L, Pacheco-Reyes F, Villarreal-Quintanilla JA, Robledo-Torres V, Encina-Domínguez J, Lara-Ramírez EE & Perez-Rodriguez M

ISSN 0215-4706 (print) | e-ISSN 2460-6944 (online) |© 2026 The Author(s). Published by BRIN Publishing
This work is licensed under a Creative Commons Attribution-NonCommercial-ShareAlike 4.0 International License. (https://creativecommons.org/licenses/by-nc-sa/4.0)

2024. Effectiveness of DNA barcodes (*rbcL, matK, ITS2*) in identifying genera and species in Cactaceae. *Pakistan Journal of Botany* 56(5): 1911–1928.

Yu G, Smith DK, Zhu H, Guan Y & Lam TTY 2017. ggtree: an R package for visualization and annotation of phylogenetic trees with their covariates and other associated data. *Methods in Ecology and Evolution* 8(1): 28–36.

Yudaputra A, Fijridiyanto IA, Yuzammi, Witono JR, Astuti IP, Robiansyah I, Hendrian R, Hutabarat P, Yuswandi AY, Raharjo PD, Syartinilia & Cropper WP 2022. Habitat preferences, spatial distribution and current population status of endangered giant flower *Amorphophallus titanum*. *Biodiversity and Conservation* 31(3): 831–854.